Seventh International colloquium on Surfaces
(Technische University Karl Marx Stadt, DDR, 1988) pp. 308-316.

WISSENSCHAFTLICHE TAGUNGEN
der Technischen Universität
Karl-Marx-Stadt 1/1988

VII. INTERNATIONALES OBERFLÄCHENKOLLOQUIUM

8. bis 10. Februar 1988 in Karl-Marx-Stadt

Band 1

Volltexte der Vorträge

For the VIIth International Colloquium on Surfaces

OPTICAL SCATTERING FROM ROUGH SURFACES: EXPERIMENT AND THEORY

T. V. Vorburger, L. X. Cao*, C. H. W. Giauque,
J. Raja*, D. E. Gilsinn, and L. Fullana*
National Bureau of Standards
Gaithersburg, MD 20899, USA

1. Introduction

Optical scattering techniques have been used to assess the surface roughness of optical components like x-ray mirror prototypes and diamond- turned parts [1,2]. Optical scattering has also been extended to the inspection of rough surfaces such as automobile and other mechanical components [3,4]. These methods are well suited for on-line roughness monitoring because they are fast, noncontacting, and can be easily integrated into an automated manufacturing system [5]. A single measurement yields a quantity that represents some average property of the surface roughness.

The main problem that prevents the widespread use of optical scattering for roughness inspection is the inability to deduce reliable roughness parameters from optical measurements. There are two main challenges. The first is the problem of determining the optical scattering model, i.e., developing a mathematical description of how light is scattered by rough surfaces. This description depends on whether the surface has a well-defined direction of machining marks (lay) or is isotropic and on whether it is optically smooth. If the surface is optically smooth, the roughness heights are much smaller than the wavelength of the optical probe and one can use a perturbation theory [6,7] to describe the scattering. Accordingly, a number of experiments have been performed for optical surfaces to compare the measured angular scattering distribution with one calculated with the perturbation theory [6,8].

By contrast, the roughness heights of many engineering surfaces are typically in the range 0.1 - 1.0 μm, that is, on the same order of magnitude as the wavelength of light. The mathematical description in this regime is more complicated [9,10] than the perturbation theory applicable to optical surfaces.

The second challenge is that of solving the inverse problem to derive surface parameters from optical scattering quantities [11,12]. Because of these difficulties, optical scattering methods for mechanical parts are almost exclusively used in an empirical way relying on the use of calibration surfaces with known roughness parameters that are similar to the unknown surfaces to be measured.

This paper primarily deals with the first problem. In order to use optical techniques to monitor roughness with a higher degree of confidence, it is essential to derive optical scattering quantities like the angular distribution or the specular intensity, from basic principles. This paper addresses the problem by applying a phase screen model for computing the optical scattering quantities. The computed distribution is compared with experimental results to check the validity of the model. One consequence of this research, together with future work on the inverse problem, may be a greater usefulness of optical techniques for evaluating surface roughness.

---

*Visiting Scholar

Angular Scattering System for Measuring Surface Roughness

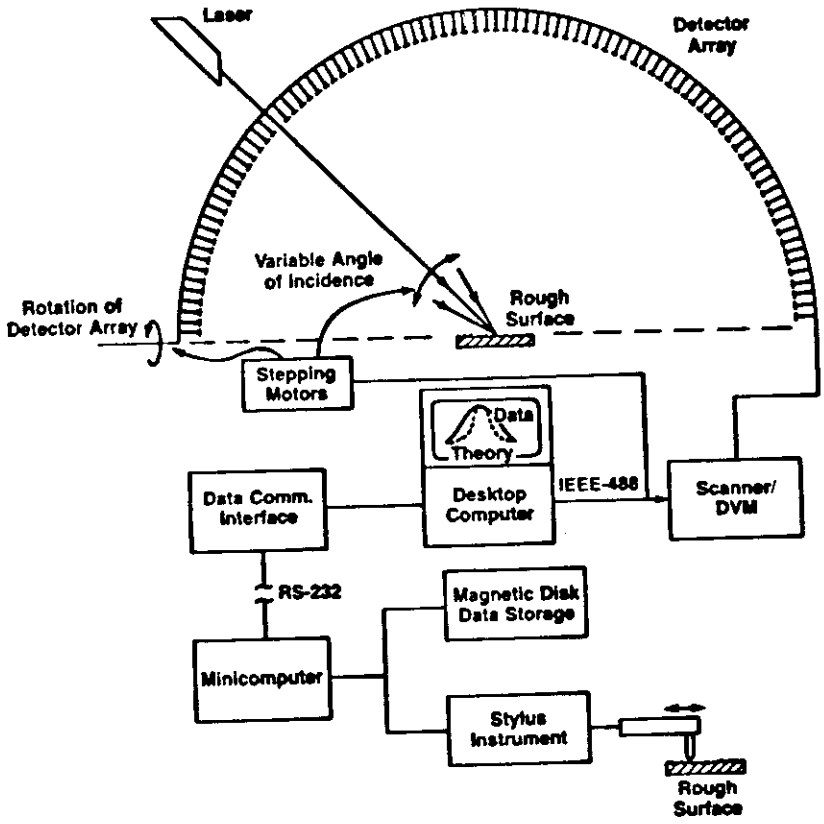

Figure 1 Block diagram of the experiment. The optical instrument, DALLAS, is shown at the top, and the stylus system, at the bottom. Experimental and computed angular distributions may be compared on the desktop microcomputer shown near the center.

2. Optical Scattering Measurement

When a beam of laser light is reflected by a rough surface, the radiation is scattered into an angular distribution according to the laws of physical optics. The intensity and pattern of the scattered radiation depend on the roughness heights, the roughness spatial wavelengths, and the wavelength of the incident light. In general, small spatial-wavelength components diffract the light into large angles relative to the specular direction and long spatial wavelength components diffract the light into small angles. For very smooth surfaces, most of the light propagates in the specular direction. As the roughness increases, the intensity of the specular beam decreases, while the diffracted radiation increases in intensity and becomes more diffuse. These phenomena are the basis for our experiments to measure optical angular scattering from rough surfaces and to predict the scattering from a knowledge of the roughness topography.

A block diagram of the experimental setup is shown in Fig. 1. It includes an optical angular scattering system named DALLAS (detector array for laser light angular scattering) [13] that consists of an illumination and detection system. A He-Ne laser beam is used to illuminate the surface. The angle of incidence may be varied by a stepping motor that controls the position of the mirrors directing the light onto the surface. The illuminated region is a spot approximately 2 mm × 3 mm in size, depending on the angle of incidence. The detection system consists of an array of 87 detectors spaced 2° apart in a semicircular yoke centered on the

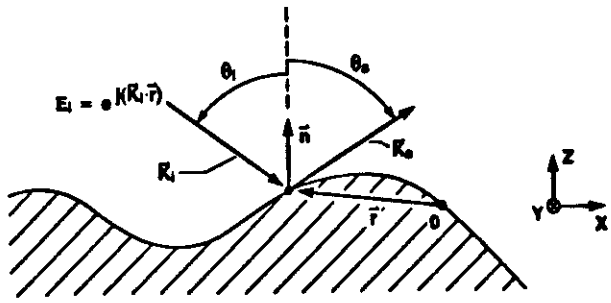

Figure 2 Schematic diagram of the scattering geometry showing the incoming plane wave with vector K_i, and angle of incidence θ_i and an outgoing wave vector K_s with scattering angle θ_s. r is the vector from the origin 0 to the point under consideration. (Vector symbols have arrows in the figure but are boldfaced in the text.)

illumination spot on the specimen. The sensitive area of each detector is a circle subtending about 1.2° at the specimen.

The yoke can be rotated about one axis by a stepping motor so that the detectors can sample almost the entire hemisphere of radiation scattered from the surface. The radiation signals collected by the detectors are routed by a scanner to an analog-to-digital (A/D) converter. The resulting angular distribution is stored in a desktop computer for eventual comparison with the computed distribution based on the developed model.

3. Stylus Measurement

A Talystep** stylus instrument interfaced to a minicomputer was used to measure the detailed surface topography. As the stylus traverses the peaks and valleys of the surface, the vertical motion is converted to a time-varying electrical signal. This electrical signal is digitized at an abscissa spacing of 0.2 μm, and the digitized profile is stored on a magnetic disk. The profile consists of 4000 points altogether, representing a profile length of 800 μm.

The horizontal resolution of the instrument is approximately 0.5 μm, limited by the width of the stylus tip and by the high frequency response of the stylus instrument controller. The ultimate vertical resolution of the stylus instrument is approximately 0.3 nm rms. In our experiment, the vertical resolution was limited by the quantization level of the A/D converter which in turn depended on the magnification scale of the stylus instrument controller. At the 10,000X magnification of our measurements, the quantization level was 1.2 nm. The stylus measurements were taken with a total of ten profiles distributed over an area of approximately 3 mm × 5 mm.

4. Theory

The model used to predict the angular scattering distributions is based on a scalar theory of light scattering investigated by Beckmann and Spizzichino [9] and others [14,15]. The theory assumes that a plane wave of uniform intensity illuminates the specimen surface and that the electric field and its normal

---

**Certain commercial equipment are identified in this report to specify adequately the experimental procedure. In no case does such identification imply recommendation or endorsement by the National Bureau of Standards, nor does it imply that the equipment identified are necessarily the best available for the purpose.

derivative at the surface can be expressed in terms of a surface reflection coefficient [9] that is independent of local surface topography. The geometry of this scattering problem is shown in Fig. 2. The surface is assumed to be two dimensional, i.e., rough in the x direction and smooth in the y direction. The incoming plane wave is represented by the wave vector K_i with angle of incidence θ_i with respect to the normal vector n of the mean plane of the surface. The functional form for the incident electric field E_i at the surface is assumed to be $\exp(jK_i \cdot r)$. The scattered electric field is to be evaluated for an angle θ_s with corresponding outgoing vector K_s. The vector r extends from some nearby origin 0 to a point on the surface.

The scattered electric field E can be calculated as a function of scattering angle θ_s in the Fraunhofer zone of the scattered radiation field. It is given by

$$E(\theta_s) = C_o F(\theta_s), \tag{1}$$

where C_o is a quantity that depends on θ_i and E_i but not on θ_s, and F contains all of the information concerning the shape of the scattering distribution as a function of θ_s. F includes the optical phase integral over the surface profile z(x) and an angular factor depending on θ_i and θ_s as follows:

$$F(\theta_s) = \frac{(1 + \cos(\theta_i - \theta_s))}{\cos\theta_i + \cos\theta_s} \int_0^L e^{jv \cdot r}\, dx \tag{2}$$

where $v = K_i - K_s$, L is the length of the illuminated region along the x direction, and $r = xi + z(x)k$. The vectors i and k are unit vectors in the x and z directions, respectively, and only $v \cdot r$ contains all of the information concerning the surface profile. In detail,

$$\begin{aligned} v \cdot r &= v_x x + v_z z(x) \\ &= 2\pi/\lambda \left[(\sin\theta_i + \sin\theta_s)x - (\cos\theta_i + \cos\theta_s)z(x)\right] . \end{aligned} \tag{3}$$

The sign convention here is that $\theta_s = -\theta_i$ in the specular scattering direction.

The investigation was carried out by first measuring the angular intensity distribution using the DALLAS detector array and then computing the theoretical intensity distribution given by $|F(\theta_s)|^2$ using the digitized surface profile data z(x) in Eq. (2). The computed distribution was compared to the measured one for different surfaces to test the adequacy of the model.

5.1 Experimental Angular Distributions

Specimens of hand-lapped stainless steel (S.S.) were studied with both the stylus and optical scattering techniques. These are listed in Table I with identification numbers, their measured rms roughness (R_q) values, and the types of S.S. from which they were made. A typical angular distribution for specimen #15 is shown by the solid curve in Fig. 3. The angle of incidence was -54° so the peak on the right hand side of the curve corresponds to the specular direction at +54°.

All of the surfaces had unidirectional roughness marks left by the hand-lapping process. The measured roughness is significantly smaller along the lapping marks than perpendicular to the marks. When the surface is oriented with the lapping marks perpendicular to the plane of incidence of the light, the reflected light is scattered into a thin wedge about the plane of incidence. Hence, the experimental scattering geometry fits the description of Sec. 4.

TABLE I

Specimens used in this study with their measured rms roughness values (R_q) and types of stainless steel.

Specimen ID	R_q (μm)	Material (S.S.)
3	0.22	Nitronic 40 (N40)
5	0.14	AF-1410
6	0.48	AF-1410
7	0.19	13-8
8	0.37	13-8
10	0.44	347
13	0.31	N40
14	0.080	N40
15	0.22	347

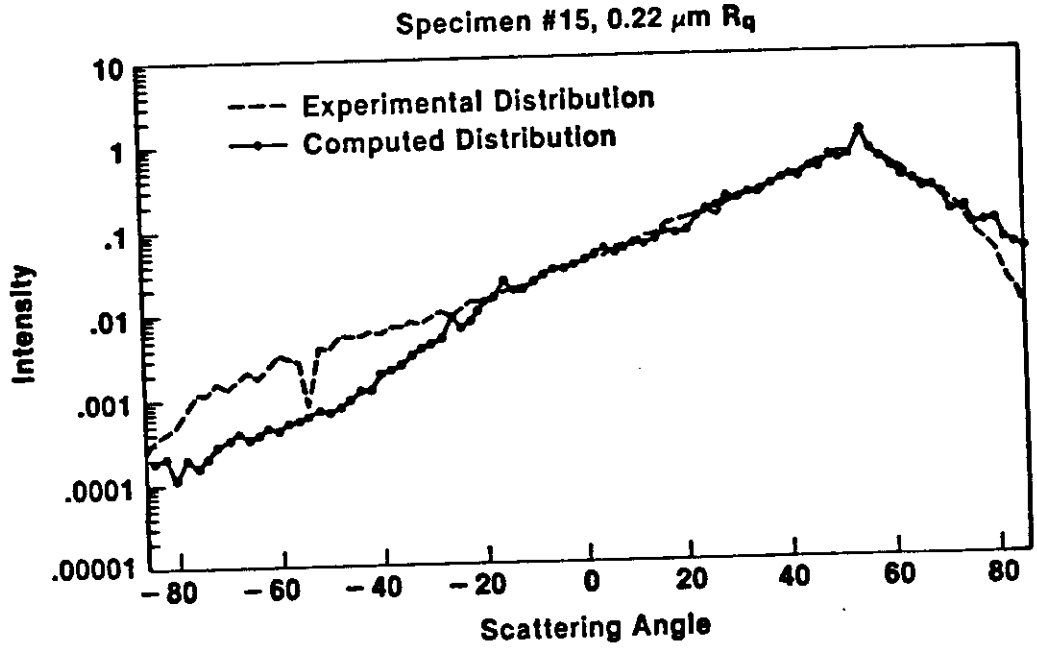

Figure 3 Experimental and computed angular scattering distributions obtained for specimen #15. The angle of incidence was -54°. The computed distribution was generated from Eq. (2) with z(x) data measured by the stylus instrument. The measured R_q was 0.22 μm.

However, a single scan of the detectors in the plane of incidence is not sufficient to collect all the angular scattering information, since some of the scattered light falls slightly out of the plane of the detector yoke located in the plane of incidence. Therefore, the intensity data were collected in five angular scans over a thin solid angle strip centered about the plane of incidence to collect all the scattered light. The intensity value at each position in Fig. 3 is a sum of five values measured in this way.

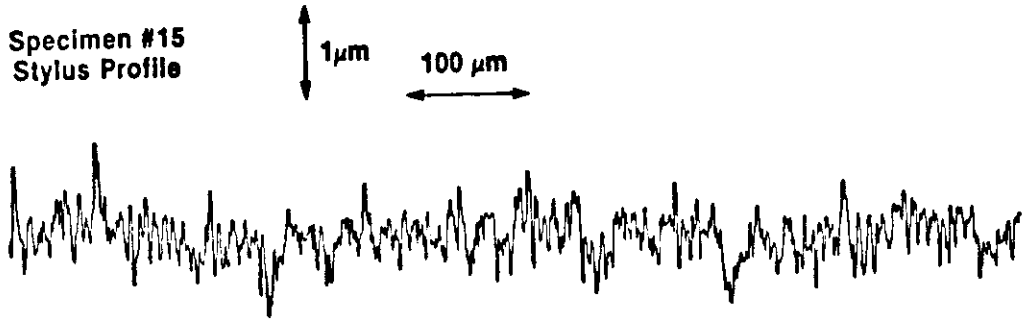

Figure 4 Surface profile for specimen #15, one of ten profiles measured with the stylus instrument for this surface.

The single sharply lower reading in the experimental data of Fig. 3 occurs at the backscattering angle of -54° when the mirror directing the incident light towards the surface also shadows one of the detectors from the scattered light.

5.2 Computed Angular Distributions

The computation uses surface profiles measured with respect to a fixed datum. A typical profile is shown in Fig. 4. The least-squares straight line was subtracted from the stored profile before substitution into Eq. (2). The least-squares line was assumed to define the mean plane that gives rise to the specular beam in the optical setup. The profile data z(x) obtained after removing the least-squares line were used in Eq. (2) to evaluate the relative field strength F, for each θ_s. From there $|F|^2$ was calculated to derive a quantity proportional to light intensity.

This quantity was then averaged to take into account speckle pattern fine structure. We performed the speckle average by calculating $|F|^2$ for closely spaced angles and summing the results. Seven angles in the plane of incidence, separated from one another by 0.05° and centered around each θ_s, were used to compute the theoretical intensity for that θ_s.

The intensity distributions resulting from the speckle average were then averaged over 10 surface profiles in order to achieve some degree of area average that simulates the area averaging of the light scattering method. As a result of the averaging procedure, the relative intensity calculated for each value of θ_s is an average of the squared absolute value of 70 integrals, each represented by Eq.(2).

5.3 Discussion

Three of the calculated distributions together with the measured distributions are shown in Figs. 3, 5, and 6. For each graph the theoretical curve is normalized so that its total intensity was the same as the experimental curve. That is, the sum of the 87 theoretical intensity values equals the sum of the 87 experimental values.

Figure 5 was taken for the roughest of the three with R_q = 0.37 μm. As a result, there is no intensity in the specular beam at +54° and all of the scattered light is diffuse.

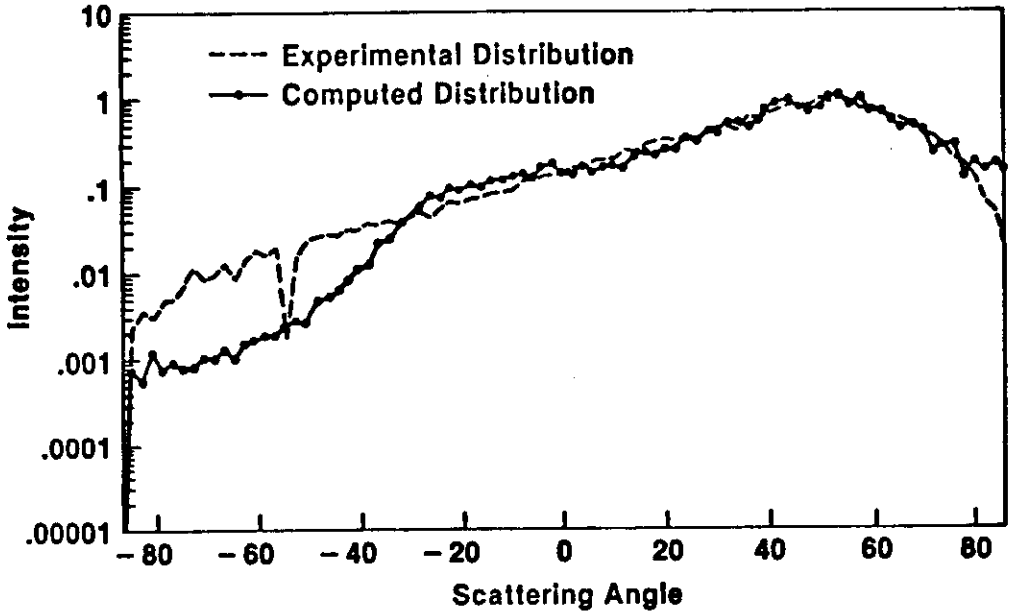

Figure 5 Experimental and computed angular distributions obtained for specimen #8. Angle of incidence = -54°. The measured R_q was 0.37 μm.

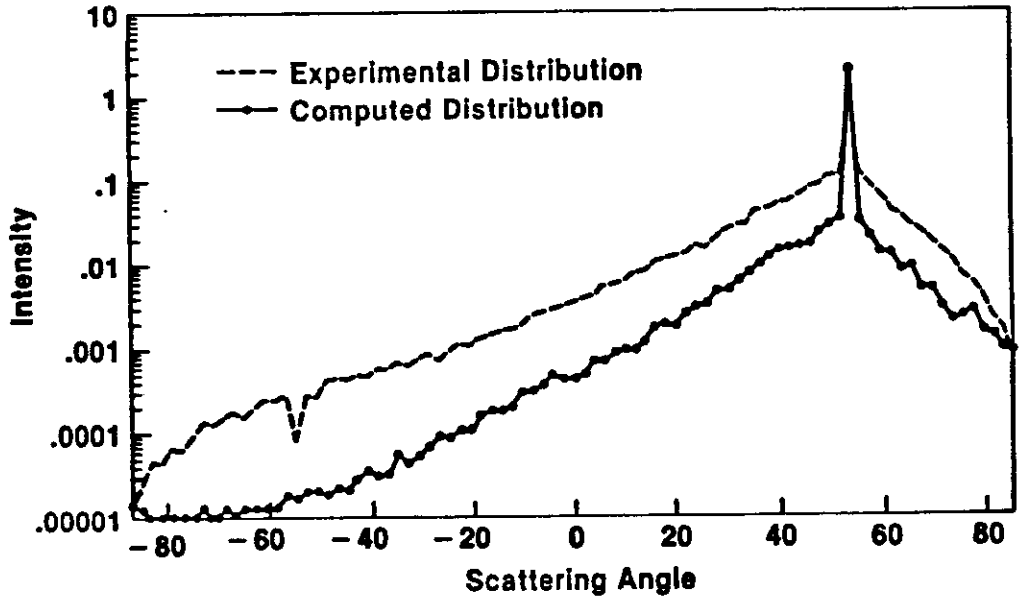

Figure 6 Experimental and computed angular distributions for specimen #14. Angle of incidence = -54°. The measured R_q was 0.080 μm.

The agreement between theory and experiment is excellent except at the large scattering angles in the left hand wing of the distribution where the theoretical results drop below the experimental ones.

The disagreement at large scattering angles may be attributed to three sources of error.

First, the approximation that we used is expected to be invalid at large scattering angles where multiple scattering and shadowing can take place. The analysis represented by Eq. (2) assumes that every point on the surface profile is uniformly illuminated and contributes to the scattering at every angle θ_s.

However, it is likely that at grazing scattering angles, the outgoing light from certain valleys is blocked by the peaks and it is also possible that some of these valleys are shadowed from the incoming beam as well. The former effect would tend to reduce the radiation scattered into the wings. The effects due to the shadowing of the incoming beam are not clear.

Perhaps more significant is the high spatial frequency limitation of the stylus instrument discussed previously. The high spatial frequency components of the surface roughness scatter the light into large scattering angles in accordance with the diffraction condition [9]. However, spatial wavelengths of about 0.5 μm and below are not well resolved by the stylus instrument. Hence, scattering intensities at large scattering angles predicted from the stylus profile $z(x)$ should be attenuated from those measured experimentally. Preliminary numerical tests using smoothed and artificially roughened surface profiles show qualitative agreement with this observation.

Finally, the assumption that the surface reflection coefficient is not a function of the local surface topography seems to be valid for these metallic surfaces. However, the difference between theory and experiment suggests a closer investigation of that assumption might be fruitful.

The data of Fig. 3 were taken from a smoother surface than those of Fig. 5. In Fig. 3, there is a small specular component that yields the sharp peak in the experimental distribution at $\theta_s = 54°$. This component also is apparent in the computed distribution, so the agreement between experiment and theory is still quite good except once again in the left hand wing of the distribution.

The measured R_q value corresponding to the data of Fig. 6 was only 0.080 μm. In this case, it is apparent that the ratio between the intensity of the specular peak and the diffuse scattering intensity is not predicted quantitatively by Eq. (2). However, the shape of the diffuse part of the theoretical scattering pattern is still similar to the experimental one since the two curves run generally parallel to one another except at the high scattering angles.

The failure of Eq. (2) to predict the ratio of specular to diffuse intensities may be due to the special nature of the specular beam itself and to difficulties with describing it quantitatively. The theory was calculated in the Fraunhofer regime of the scattering field where the distance from the illumination spot to the detectors is assumed to be infinite [9]. This assumption leads to a simplification of both the scattering geometry and of the exponential phase factor in Eq. (2).

In fact, the detectors are located on a radius of 164 mm. Therefore, the calculation of specular beam intensity should be checked using the Fresnel approach, where the relationship between the detector distance, the illumination spot size, and the laser wavelength would be properly accounted for.

6. Conclusion

The use of optical scattering techniques for reliable assessment of surface finish will be facilitated when scattering quantities can be predicted from theoretical models. The model reported in this paper and the good agreement obtained between theory and experiment is a step towards eliminating comparator methods presently adopted to evaluate finish using optical techniques. The analysis may now be extended to three-dimensional surfaces and the solution of the inverse scattering problem may also be attempted to obtain surface roughness parameters like R_q. The results reported in this paper take us a step closer to the quantitative prediction of surface parameters from optical scattering data, and that could lead to more widespread use of optical techniques to characterize surfaces.

7. References

1. Zombeck, M.V.; Wyman, C.C.; Weisskopf, M.C. High resolution x-ray scattering measurements for Advanced X-Ray Astrophysics Facility (AXAF), in Radiation Scattering in Optical Systems, Proc. SPIE 257, 230 (1980).

2. Church, E.L.; Jenkinson, H.A.; Zavada, J.M. Measurement of the finish of diamond turned metal surfaces by differential light scattering, Opt. Eng. 16, 360 (1977).

3. Gardner, C.S.; Alster, L.G. Electro-optic gauge for measuring the surface roughness of crankshaft bearings, Presented at the 2nd Int. Prec. Eng. Seminar, NBS, Gaithersburg, MD, May 1983; Gardner, C.S., Streight, W.E., U.S. Patent No. 4,364,663, 12/82.

4. Brodman, R.; Gerstorfer, O.; Thurn, G. Optical roughness measuring instrument for fine-machined surface, Opt. Eng. 24, 408 (1985).

5. Moncarz, H.; Vorburger, T.V. Implementation of the SRI Controller (to be published).

6. Elson, J.M.; Bennett, J.M. Vector scattering theory, Opt.Eng. 18, 116 (1979).

7. Church, E.L.; Jenkinson, J.A.; Zavada, J.M. Relationship between surface scattering and microtopographic features, Opt. Eng. 18, 125 (1979).

8. Elson, J. M.; Rahn, J. P.; Bennett, J. M. Light scattering from multilayers optics: Comparison of theory and experiment, Appl.Opt. 19, 669 (1980).

9. Beckmann, P.; Spizzichino, A. The Scattering of Electromagnetic Waves from Rough Surfaces, Pergamon, New York (1963).

10. Teague, E.C.; Vorburger, T.V.; Maystre, D.M. Light scattering from manufactured surfaces, CIRP Annals 30, 503 (1981).

11. Baltes, H.P. Topics in Current Physics: Inverse Scattering Problems in Optics, Vol. 20, Springer, Berlin (1978).

12. Roger, A.; Maystre, D. Inverse scattering method in electromagnetic optics: Application to diffraction gratings. J. Opt. Soc. Am. 70, 1483 (1980).

13. Vorburger, T.V.; Teague, E.C.; Scire, F.E.; McLay, M.J.; Gilsinn, D.E. Surface roughness studies with DALLAS - detector array for laser light angular scattering, J. Res. of NBS 89, 3 (1984).

14. Bass, F.G.; Fuks, I.M. Wave Scattering from Statistically Rough Surfaces, Pergamon, London (1979).

15. Wirgin, A. Scattering from sinusoidal gratings: an evaluation of the Kirchoff approximation, J. Opt. Soc. Am. 73, 1028 (1983).